Screening and characterization of proteorhodopsin color-tuning mutations in Escherichia coli with endogenous retinal synthesis

ARTICLE *in* BIOCHIMICA ET BIOPHYSICA ACTA · JULY 2008

Impact Factor: 4.66 · DOI: 10.1016/j.bbabio.2008.03.010 · Source: PubMed

4 AUTHORS, INCLUDING:

Leonid S Brown
University of Guelph
108 PUBLICATIONS **4,487** CITATIONS

SEE PROFILE

Biochimica et Biophysica Acta 1777 (2008) 504–513

Contents lists available at ScienceDirect

Biochimica et Biophysica Acta

journal homepage: www.elsevier.com/locate/bbabio

Screening and characterization of proteorhodopsin color-tuning mutations in *Escherichia coli* with endogenous retinal synthesis ☆

So Young Kim [a], Stephen A. Waschuk [b], Leonid S. Brown [b], Kwang-Hwan Jung [a,*]

[a] Department of Life Science and Interdisciplinary Program of Integrated Biotechnology, Sogang University, Shinsu-Dong 1, Mapo-Gu, Seoul, 121-742, Korea
[b] Department of Physics, University of Guelph, Ontario, Canada N1G 2W1

ARTICLE INFO

Article history:
Received 7 January 2008
Received in revised form 8 March 2008
Accepted 13 March 2008
Available online 27 March 2008

Keywords:
Proteorhodopsin
Spectral tuning
Membrane protein
Proton pumping
Random mutagenesis

ABSTRACT

Proteorhodopsin is photoactive 7-transmembrane protein, which uses all-*trans* retinal as a chromophore. Proteorhodopsin subfamilies are spectrally tuned in accordance with the depth of habitat of the host organisms, numerous species of marine picoplankton. We try to find residues critical for the spectral tuning through the use of random PCR mutagenesis and endogenous retinal biosynthesis. We obtained 16 isolates with changed color by screening in *Escherichia coli* with internal retinal biosynthesis system containing genes for beta-carotene biosynthesis and retinal synthase. Some isolates contained multiple substitutions, which could be separated to give 20 single mutations influencing the spectral properties. The color-changing residues are distributed through the protein except for the helix A, and about a half of the mutations is localized on the helices C and D, implying their importance for color tuning. In the pumping form of the pigment, absorption maxima in 8 mutants are red-shifted and in 12 mutants are blue-shifted compared to the wild-type. The results of flash-photolysis showed that most of the low pumping activity mutants possess slower rates of M decay and O decay. These results suggest that the color-tuning residues are not restricted to the retinal binding pocket, in accord with a recent evolutionary analysis.

1. Introduction

Proteorhodopsin (PR) is a type I retinal binding protein [1,2], which was identified by metagenomic analysis of marine γ-proteobacteria [3,4]. After the first PR was identified in SAR86 group of γ-proteobacteria [3], numerous proteorhodopsin variants were isolated from γ-proteobacteria and α-proteobacteria in Monterey Bay, Hawaii Ocean Time (HOT), Palmer station (Antarctica) [4], Mediterranean Sea, Red Sea [5], Sargasso Sea [6], and global ocean surface from eastern North American coast to the equatorial Pacific [7].

Based on the absorption maxima, there are several subfamilies of PRs with the spectral range spanning from blue (490 nm) to green (525 nm) [8]. Their distribution was shown to be stratified with depth — green absorbing pigments (GPR) at the surface and blue absorbing pigments (BPR) in deeper waters [4]. Spectroscopic analyses indicate that a substantial spectral tuning can be achieved by a single amino acid replacement [8]. Two major PR subfamilies, GPR and BPR, show more than 78% amino acid sequence identity. With structural modeling comparisons and mutagenesis, a single residue difference in the retinal binding pocket at the position 105 (Leu in GPR and Gln in BPR) was found to function as a spectral tuning switch and to account for most of the spectral difference between the two pigment families. Two mutations by which residues at the position 105 were interchanged (GPR L105Q and BPR Q105L) almost completely interconverted the absorption spectra of BPR and GPR. This single-residue switch mechanism might be the major determinant of proteorhodopsin wavelength regulation thought to be optimized to match the quality of light that reaches the depth where the bacteria thrive [8]. In addition, it has been reported that many other amino acid residues from the retinal binding pocket and elsewhere participate in spectral fine tuning in PR, similar to SR [9,10].

PR uses all-*trans* retinal as a chromophore. One of the most notable distinguishing properties of retinal among chromophores used in photosensory receptors is a large variation in its absorption spectrum depending on interactions with the apoprotein [11,12]. Protonated retinal Schiff base exhibits an absorption maximum of 440 nm in methanol but it shifts to much longer wavelength in protein microenvironment [13]. All-*trans*-retinal is produced by the central cleavage of the 15,15′ C=C bond of β-carotene [1], and one molecule of β-carotene yields two molecules of retinal. This enzymatic cleavage depends on molecular oxygen and, since no cofactors are required, the enzyme was termed 15,15′-β-carotene-dioxygenase [14]. It seems that some proteobacteria can synthesize β-carotene and convert it to

Abbreviations: PR, proteorhodopsin; GPR, green-absorbing PR; BPR, blue-absorbing PR; SR, sensory rhodopsin from halobacteria; BR, bacteriorhodopsin; DDM, *n*-dodecyl-β-D-maltoside; β-diox, 15,15′-β-carotene dioxygenase

☆ This work was supported by the Korea Research Foundation Grant (KRF 2004-042-C00113), KOSEF (F01-2005-000-10096-0), and Seoul Research and Business Development Program (10816) to K.H. Jung, and grants from NSERC and PREA to L.S. Brown. S.Y. Kim was supported by the 2nd stage of Brain Korea 21 graduate Fellowship Program.

* Corresponding author. Tel.: +82 02 705 8795; fax: +82 02 704 3601.
E-mail address: kjung@sogang.ac.kr (K.-H. Jung).

0005-2728/$ – see front matter © 2008 Elsevier B.V. All rights reserved.
doi:10.1016/j.bbabio.2008.03.010

retinal similar to eucaryotes, using the enzyme encoded by the *blh* gene to produce functionally active PR [15,16].

Like bacteriorhodopsin (BR), PR is a light-driven proton pump [3,17,18]. The two most important residues for its function are Asp-97 serving as a proton acceptor and Glu-108 serving as a cytoplasmic proton donor to the Schiff base. These two residues are homologous to Asp-85 and Asp-96 of BR [18,19]. In almost all type I rhodopsins, possibly excluding ASR, the functional photoisomerization of the retinal chromophore is from all-*trans* to 13-*cis* [1], and PR is not an exception. The photocycle intermediates of PR are similar to those of BR and are consistent with its proton transporting function [19]. The photocycle of PR contains at least five intermediates termed K, M1, M2, N, and PR'(O) [17,20]. The pumping rhodopsins are characterized by a typical photocycle turnover of <30 ms, whereas sensory rhodopsins are slow-cycling pigments with photocycle halftime typically >300 ms [1,2]. Studies of PR based on recombinant DNA and *in vitro* biochemical analyses showed a relatively fast photocycle and a robust proton pumping activity. Recently, PR-containing α-proteobacteria from SAR11 group [21] and flavobacteria [22] were cultured and photochemical properties of PR in the native membranes were measured, which may give an opportunity to discover the *in vivo* function of PR.

In order to identify additional residues important for the spectral tuning in PR, we constructed an endogenous retinal synthesis system in *Escherichia coli*, which allows for an easy screening of colored colonies depending on spectral property of the expressed rhodopsin. We identified and characterized 20 color-tuning single mutations, which are not limited to the retinal binding pocket, in agreement with a recent evolutionary analysis [10].

2. Materials and methods

2.1. Bacterial strains and plasmids

E. coli DH5α was used for cloning the mutant proteorhodopsin genes. The transformants were grown in LB (Luria–Bertani) medium in the presence of ampicillin (50 μg/mL) (USB Corp., USA) at 35 °C. All the mutants were expressed in *E. coli* strains UT5600 and β/UT for proton pumping measurements and absorption spectroscopy, respectively. *E. coli* β/UT was constructed by transforming UT5600 with a plasmid pORANGE [23], which provided an ability to synthesize β-carotene.

The plasmid pKJ900 carrying a 15,15′-β-carotene dioxygenase gene from mouse (*β-diox*) between NcoI and PmeI sites and the PR gene (Monterey Bay proteorhodopsin, MBP) between NdeI and NotI sites was used (Fig. 1). Proteorhodopsins were expressed under the lacUV5 promoter and *β-diox* was expressed under P_{BAD} promoter in *E. coli* strains UT5600 and β/UT.

2.2. PCR mutagenesis

The pKJ900 plasmid encoding C-terminally 6-His-tagged MBP (Monterey Bay Proteorhodopsin, GPR) was used as a template for random mutagenesis. MBP gene was mutagenized with *Taq* polymerase (Dae Myung Science, Korea) under condition of reduced fidelity by adding 0.05 mM $MnCl_2$ to the reaction mixture [24,25].

The PCR was performed for 30 cycles at 95 °C for 1 min, 55 °C for 1 min, and 72 °C for 2 min. The conditions for this random mutagenesis usually produce 1 mutation per 1000 base pairs, but sometimes two to three mutations were observed simultaneously. In this case we used site directed mutagenesis to separate each single mutation using the two-step mega primer PCR method [26] with *Pfu* polymerase in order to identify which site is responsible for the changed phenotype.

2.3. Expression and purification of proteorhodopsin

For proton pumping measurements, overnight cultures of each mutant in UT5600 were diluted 1:100 and grown to produce an absorbance of 0.4 OD units at 600 nm at 30 °C. Cells were induced with 5 ~ 10 μM all-*trans*-retinal (Sigma, USA) and 1 mM IPTG (Applichem, USA) for 6 h at 30 °C. For absorption spectroscopy, β/UT cells were induced with 1 mM IPTG and 0.2% (+)-L-arabinose (Sigma) for 24 h at 30 °C. Induced cells were harvested and suspended in 50 mM Tris (pH 7.0) and 150 mM NaCl. Cells were lysed by sonication (Branson sonifier 250) at 4 °C followed by low-speed (3220 ×*g* for 20 min) centrifugation (Eppendorf centrifuge 5810R) to remove cell debris. Finally, cell membranes with rhodopsins were sedimented at 95,000 ×*g* for 1 h at 4 °C (Ti70 rotor, Beckman XL-90 ultracentrifuge) and the pellets were resuspended in 50 mM Tris (pH 7.0) and 150 mM NaCl.

The rhodopsins were extracted from the membrane by incubating with 1% n-dodecyl-β-D-maltopyranoside (DDM) (Anatrace, USA), 50 mM Tris (pH 7.0), and 150 mM NaCl overnight at 4 °C. Unsolubilized material was removed by centrifugation at 30,000 ×*g* for 15 min at 4 °C (Ti70 rotor, Beckman XL-90 ultracentrifuge). The supernatant was mixed with Ni^{2+}-NTA agarose (Qiagen) and incubated with low speed shaking overnight at 4 °C. The mixture was washed with 20 bed volumes of 25 mM imidazole (Sigma, USA) and eluted with 250 mM imidazole in the same buffer containing 0.02% DDM. The colored fraction was collected and concentrated with Amicon Ultra-4 10,000 MWCO centrifugal filter (Millipore, USA) in order to remove imidazole and concentrate the purified PR.

2.4. Immunoblot assay

Whole cell lysates containing 40 μg of protein were prepared. Quantity of proteins was determined with Bio-Rad D_c protein assay kit. Anti 6×HN polyclonal antibody (Clontech, USA) at a 1:6000 dilution was used as the primary antibody, and HRP conjugated goat anti-rabbit IgG antibody (Santa Cruz) at a 1:15,000 dilution was used as the secondary antibody. Reactive bands were visualized with Western Lightning Chemiluminescence Reagent Plus (PerkinElmer Life Science, USA).

2.5. Absorption spectroscopy and pK_a measurements

The absorption spectra of mutants were recorded at pH 4.0, 7.0, and 10.0 with Shimadzu UV-visible spectrophotometer (UV-2550). Difference spectroscopy was

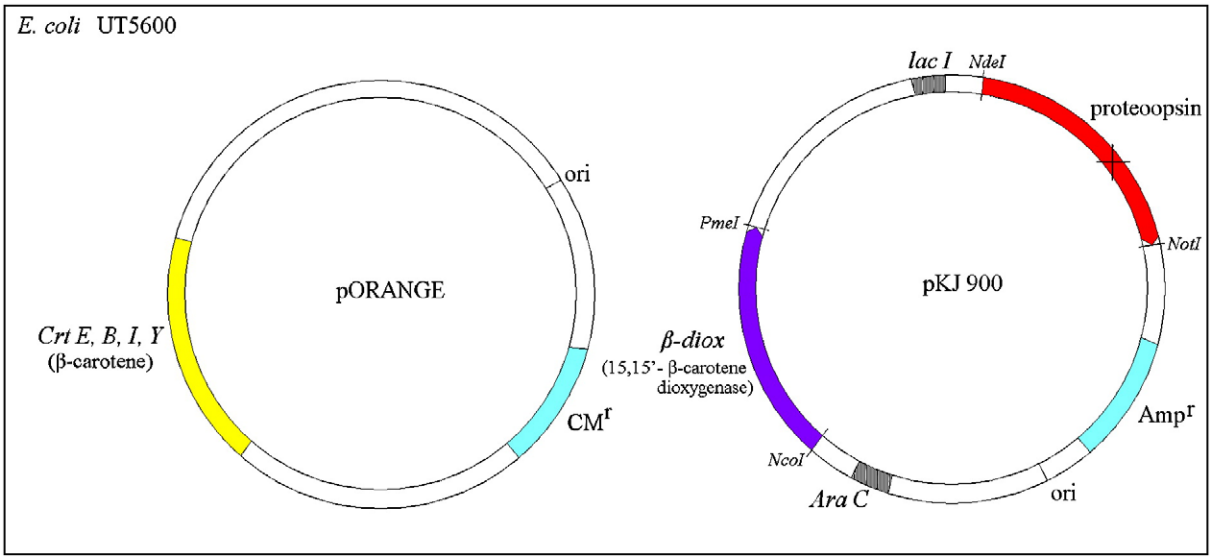

Fig. 1. *E. coli* β/UT5600 strain was constructed by transformation of pORANGE plasmid for β-carotene synthesis into *E. coli* UT5600 strain. The pKJ 900 plasmid contains Monterey Bay proteorhodopsin (MBP) gene and mouse *dioxygenase* gene which could produce all-*trans* retinal from β-carotene. The dioxygenase gene is under arabinose promoter and the opsin gene is under lacUV5 promoter. Randomly mutagenized proteoopsin gene was inserted into the pKJ900 and transformed into *E. coli* β/UT for protein expression.

performed with the His-tagged WT and mutant proteorhodopsins after the purification using Ni^{+2}-NTA column. For calculating the pK_as of the Schiff base counterion, the difference spectra were measured from pH 4.0 to pH 10.0 using the spectrum at pH 7.0 as the reference and titration curves were constructed. The corrected ratio of protonated and unprotonated forms at different pH values was determined and fitted with standard functions ($y = A/(1+10^{pH-pKa})$) [27].

2.6. Proton pumping measurements

The 500 mL cultures of induced cells were harvested by centrifugation at 3220 ×g for 20 min (Eppendorf centrifuge 5810 R) and suspended in 10 mL of buffer I (30 mM Tris–HCl, pH 8.0, and 20% sucrose). 100 μg of lysozyme was added and stirred at room temperature for 20 min. The treated cells were collected by centrifugation at 3220 ×g for 15 min at room temperature. Spheroplasts were resuspended in 400 μL of buffer II (100 mM KPi, pH 7.0, 20 mM $MgSO_4$, 20% sucrose, 1.6 mg of DNase I) and injected using a 3 mL syringe (26 gauge needle) into 200 mL of rapidly stirring solution I (50 mM KPi, pH 7). After 15 min at 37 °C in the shaking incubator, Na_2-EDTA was added to a final concentration of 10 mM. After another 15 min, $MgSO_4$ was added to a final concentration of 15 mM, followed by 15 min incubation. Spheroplast vesicles were collected at 30,778 ×g for 1 h at 4 °C (Ti70 rotor, Beckman XL-90 ultracentrifuge) and washed with 10 ml solution II (10 mM NaCl, 10 mM $MgSO_4 \cdot 7H_2O$, 100 μM $CaCl_2$) and resuspended in 3 ml of solution II [27]. Samples were illuminated through the short wavelength cutoff filter (Sigma Koki SCF-50S-44Y, Japan) and the pH changes were monitored (Horiba pH meter F-51). The pH data were transferred and recorded automatically with Horiba data Navi program.

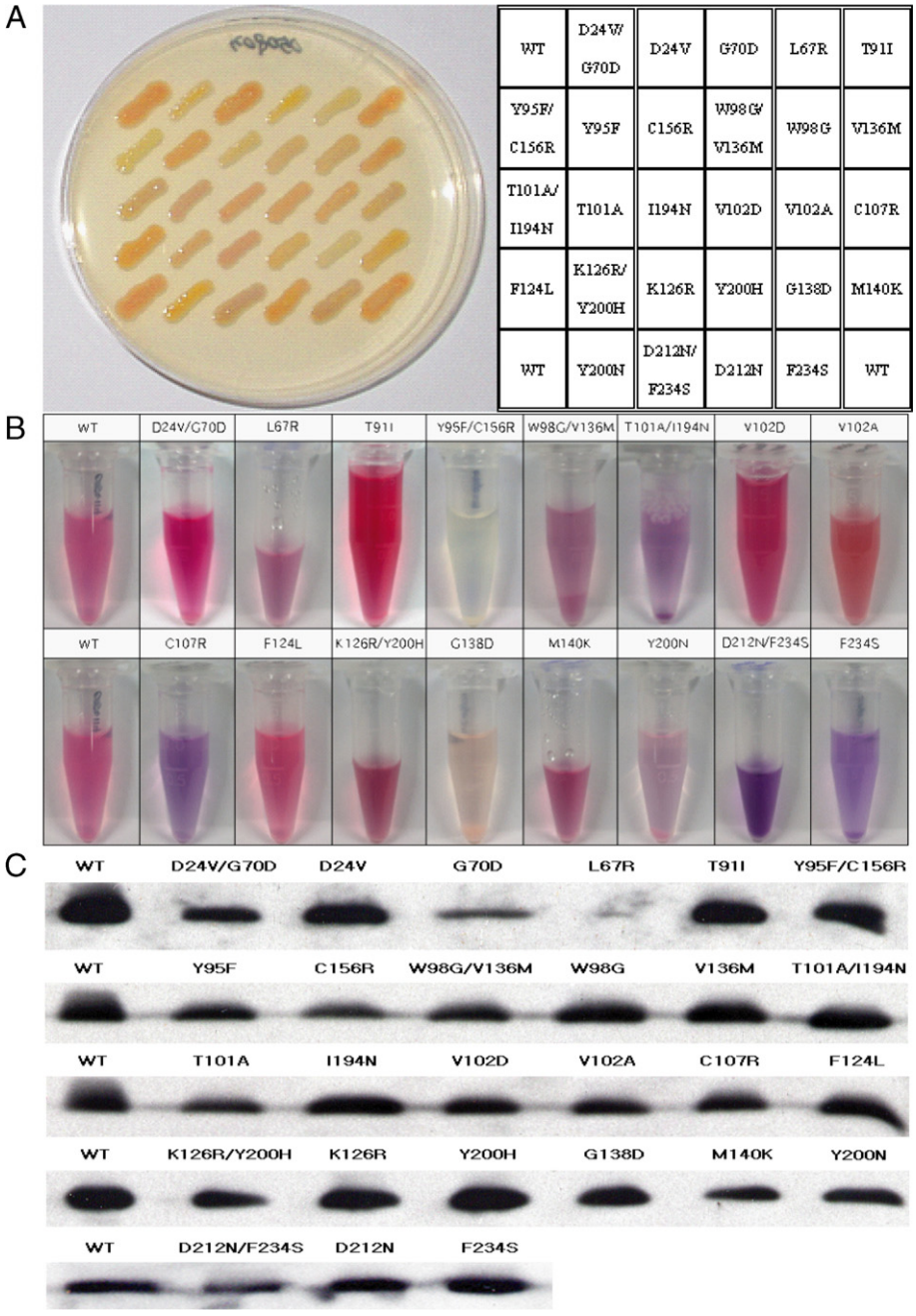

Fig. 2. Screening of proteorhodopsin mutants. A. Colonies of *E. coli* β/UT strain in which mutant proteorhodopsins are expressed were patched on the LB agar plate with ampicillin, chloramphenicol, IPTG, and L-arabinose. Each of the mutants showed a color different from the wild type. The table indicates the amino acid sequence changes of the mutants. B. Each tube contains purified mutant proteorhodopsin in 50 mM Tris, pH 7.0, 150 mM NaCl, and 0.02% DDM. C. Immunoblot analysis of His-tagged PR mutants in *E. coli*. An identical amount of membrane protein in each lane (40 μg) was separated by SDS PAGE. The immunoblot used anti-His-tag antibody. Most of the mutant proteins were expressed at a level similar to that of the wild-type. However, the expression level of D24V/D70D, C156R, T101A, V102D, V102A, K126R/Y200H, M140K, and D212N/F234S was somewhat lower. The L67R and G70D mutants were expressed more weakly, so we concentrated the proteins from a larger culture.

2.7. Photocycle measurements

The samples for time-resolved laser spectroscopy were prepared as described elsewhere [19]. Briefly, DDM treatment of the pelleted membranes followed by sequential centrifugations (at low speed to remove large membrane aggregates and at high speed to remove solubilized material) yielded clear suspensions of membranes containing PR, which were encased in polyacrylamide gels. The gels were washed and soaked in appropriate buffers for at least 2 h. Time-resolved laser spectroscopy in the visible range (flash-photolysis) was performed on our custom-built apparatus [28]. Photocycle excitation was provided by the second harmonic of an Nd-YAG laser (Continuum Minilite II) using ~7 ns pulses at 532 nm. Absorption changes of monochromatic light (provided by an Oriel QTH source and two monochromators) were followed using an Oriel photomultiplier with 350 MHz wide-bandwidth amplifier and a Gage AD converter (CompuScope 12100-64M). The kinetic traces were converted into a quasilogarithmic time-scale using homemade software for kinetics analysis.

3. Results

3.1. Isolation of color-tuning mutants

Proteorhodopsin genes randomly mutagenized by PCR were transformed into *E. coli* β/UT strain capable of β-carotene synthesis [23]. All-*trans* retinal is provided to PR internally from β-carotene by mouse 15,15′-β-carotene dioxygenase (Fig. 1). The cells expressing PR formed colored colonies on the LB agar plates containing ampicillin (50 μg/mL), chloramphenicol (34 μg/mL), 1 mM IPTG, and 0.2% L-arabinose (Fig. 2A). Fifty three out of 775 (6.8%) single colonies with changed color (compared to the wild type) were isolated by visual inspection; those included 22 yellow colored colonies. Finally, we obtained 16 isolates and figured out the positions of mutations by DNA sequencing. Six isolates had more than one mutation in the MBP gene, so we had to separate them by site-directed mutagenesis and in the end we characterized 27 single and double mutants. Six of yellow colored mutants have nonsense mutations, a stop codon in the middle of the gene (the mutated residues were W74, S89, R94, W98, K126, W197), so that PR could not be expressed. The majority of mutagenized residues (more than a half) are localized on helices C and D, and the rest of them are spread through the rhodopsin, except for the helix A (Fig. 3). Interestingly, only four mutations were localized in the putative retinal binding pocket, even though it should be noted that our method may not produce the exhaustive set of all color-affecting residues.

3.2. Spectral characterization of color-tuning mutants

All of the color-tuning mutants (except for the nonsense mutants) and the wild-type PR were expressed in *E. coli* β/UT strain on a larger scale for spectral characterization. Expression levels of T101A (67%), K126R/Y200H (78%), and D212N/F234S (81%) mutants were somewhat lower than that of the wild-type (Fig. 2C). L67R and G70D mutants were expressed weakly, so those proteins were concentrated 2-4 times from large-scale culture for characterization. Protein expression level of D24V/G70D, C156R, V102A, V102D, and M140K was also a little lower than that of wild-type. For C156R and M140K, we collected more membranes and concentrated them for the spectral measurements as they easily bleached to yellow color in detergent.

We purified the wild-type and mutant PRs with C-terminal 6-His tag in non-denaturing detergent DDM (*n*-dodecyl-β-D-maltopyranoside) using Ni^{2+}-NTA resin. The final concentration of DDM in which the proteins were solubilized was 0.02%. The colors of the purified mutant pigments were very diverse and different from the colors of the respective colonies on the plate (Fig. 2A and B). The possible reasons for the latter difference are: i) the color of accumulated β-carotene masks that of the pigments on the plate; ii) the expression level is different for each colony; iii) microbial rhodopsins tend to blue-shift upon solubilization.

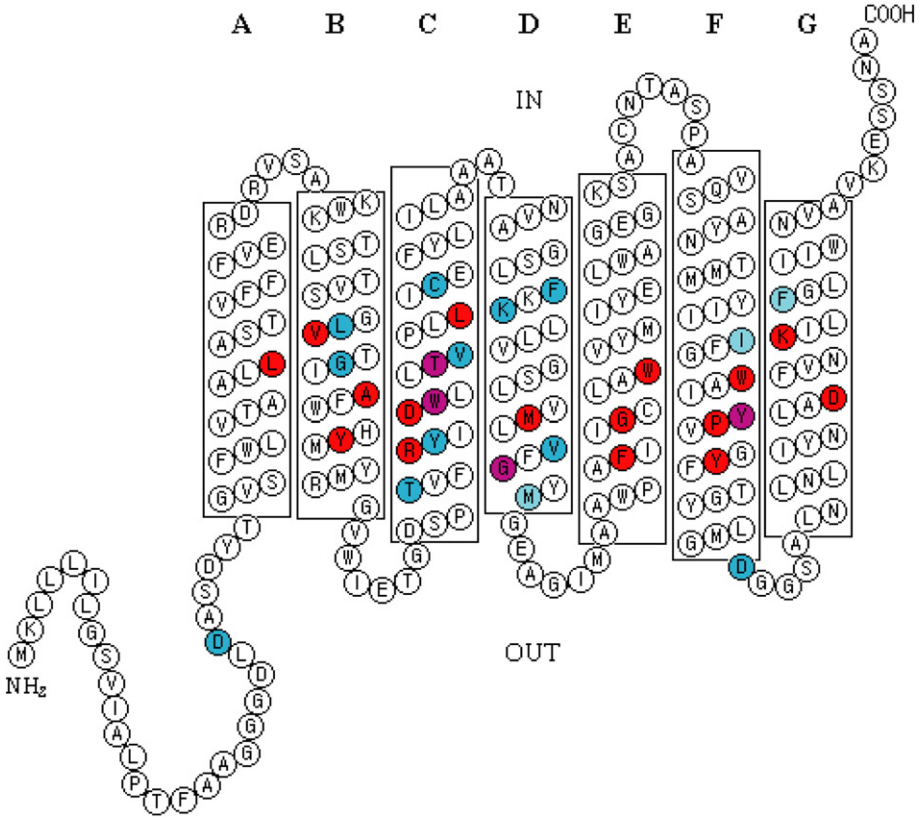

Fig. 3. Two-dimensional model of proteorhodopsin. Single letter amino acid codes are used. The transmembrane topology is based on the crystallographic structure of bacteriorhodopsin (BR) and the multiple sequence alignment of microbial rhodopsins [2]. Predicted retinal binding pocket residues are marked in red, and mutation sites which affect the absorption maxima are marked in blue. The purple marks the mutated residues in the retinal binding pocket. In total, 18 positions were influencing the absorption maximum at high pH. More than a half of the mutations are located on helices C and D, and four mutations are in the retinal binding pocket.

Table 1
The pK_a values from spectroscopic pH-titrations, absorption maxima, the half-times of the decay of the major photocycle intermediates and pumping activity of proteorhodopsins

#	Name	Mutation	pK_a	λmax$_{acid}$	λmax$_{alkaline}$	M decay	O decay	Pumping
	Wild type		7.3	548 nm	520 nm	10 ms	48 ms	+++
1	D24V/G70D		8.1	547 nm	523 nm	ND	ND	+
	D24V	GAU (D) → GUU (V)	6.8	548 nm	521 nm	5 ms	20 ms	++
	G70D	GGU (G) → GAU (D)	8.2	547 nm	518 nm	ND	ND	+
2	L67R	CUU (L) → CGU (R)	7.6	558 nm	547 nm	ND	ND	+
3	T91I	ACU (T) → AUU (I)	7.1	540 nm	518 nm	3 ms	8 ms	++
4	Y95F/C156R		ND	ND	ND	ND	ND	ND
	Y95F	UAC (Y) → UUC (F)	6.3	524 nm	513 nm	ND	20 ms	++
	C156R	UGU (C) → CGU (R)	7.0	545 nm	520 nm	ND	ND	+
5	W98G/V136M		7.6	531 nm	509 nm	ND	ND	++
	W98G	UGG (W) → GGG (G)	7.7	503 nm	493 nm	ND	ND	+
	V136M	GUG (V) → AUG (M)	7.0	549 nm	518 nm	4 ms	23 ms	++
6	T101A/I194N		8.0	568 nm	538 nm	37 ms	240 ms	+
	T101A	ACA (T) → GCA (A)	7.5	564 nm	533 nm	164 ms	88 ms	+
	I194N	AUC (I) → AAC (N)	7.6	551 nm	522 nm	5 ms	36 ms	++
7	V102D	GUU (V) → GAU (D)	6.9	548 nm	518 nm	6 ms	24 ms	++
8	V102A	GUU (V) → GCU (A)	7.2	538 nm	514 nm	15 ms	199 ms	+
9	C107R	UGU (C) → CGU (R)	8.4	551 nm	540 nm	18 ms	1610 ms	+
10	F124L	UUU (F) → CUU (L)	6.8	542 nm	524 nm	19 ms	30 ms	++
11	K126R/Y200H		7.2	532 nm	502 nm	14 ms	130 ms	+
	K126R	AAA (K) → AGA (R)	7.5	551 nm	522 nm	4 ms	31 ms	++
	Y200H	UAU (Y) → CAU (H)	7.6	524 nm	497 nm	16 ms	98 ms	++
12	G138D	GGU (G) → GAU (D)	7.4	493 nm	510 nm	ND	ND	++
13	M140K	AUG (M) → AAG (K)	7.6	556 nm	518 nm	ND	ND	+
14	Y200N	UAU (Y) → AAU (N)	7.9	531 nm	505 nm	198 ms	2230 ms	+
15	D212N/F234S		8.0	562 nm	537 nm	7 ms	260 ms	++
	D212N	GAC (D) → AAC (N)	6.8	548 nm	518 nm	4 ms	20 ms	+++
	F234S	UUU (F) → UCU (S)	7.9	562 nm	539 nm	9 ms	290 ms	+
16	F234S	UUU (F) → UCU (S)	7.9	562 nm	539 nm	9 ms	290 ms	+

ND indicates that the photocycle could not be measured due to the instability of DM-treated PR mutant or a certain intermediate could not be observed. Also, the spectral properties, the photocycle and pumping activty of Y95F/C156R were not determined because the mutant was not able to produce a colored pigment in the *E. coli* expression system. Relative proton pumping activity is shown by +++ (>0.15 $\Delta[H^+]\times10^{-9}$), ++ (0.05–0.15), and + (≤0.05/10 s) as indicated in Fig. 6.
# indicates the number of a mutant isolated from colonies with changed color. ND, Not Determined.

Absorption maxima and pK_a values of titratable groups (mostly, the Schiff base counterion) of each purified pigment was measured (Table 1). Microbial rhodopsins in general exhibit two spectral forms in a proton dependent equilibrium [27], so the absorption maximum of each pigment was measured in acidic state (pH 4.0) and alkaline state (pH 10.0). Absorption maxima of ten out of the twenty six expressed color-tuning mutants, D24V/G70D (minor shift), L67R, T101A/I194N, T101A, I194N (minor shift), C107R, F124L, K126R (minor shift), D212N/F234S, and F234S are red shifted, and 13 mutants, G70D (minor shift), T91I (minor shift), Y95F, W98G/V136M, W98G, V136M (minor shift), V102D (minor shift), V102A, K126R/Y200H, Y200H, G138D, M140K (minor shift), Y200N, and D212N are blue shifted when compared with the pumping (alkaline, pH 10.0) state of the wild type. One mutant, Y95F/C156R, did not produce a pigment. Fig. 4 shows absorption maxima of WT and representative mutant PRs. The pK_a values were extracted with Origin 6.0 program from pH dependent difference absorption spectra of each mutant. The spectra and pH titration curves of the wild-type and representative mutant proteins are shown in Fig. 5.

3.2.1. Mutations in the N-terminus, and the helices A and B

The difference in the absorption maxima between the wild type and D24V/G70D was just 3 nm at pH 10.0. But the D24V/G70D mutant had a changed pK_a value of 8.1 (7.3 in WT). We studied the effects of the single mutations in the double mutant using site-directed mutagenesis to determine the key amino acid that contributed to the spectral and the pK_a changes in the D24V/G70D mutant. It seemed that the D24V mutation (in the N-terminus) did not contribute to the λ_{max} shift of the double mutant, because the absorption maxima of D24V were similar to the wild-type. On the other hand, the pattern of the pH-dependent difference spectra and the pK_a value of G70D (in the helix B) were analogous to the double mutant. Absorption

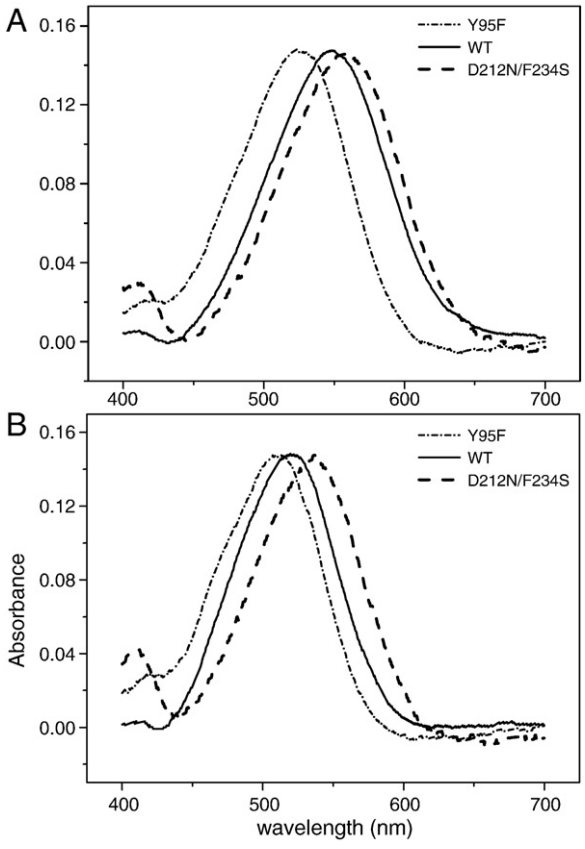

Fig. 4. Absorption spectra of purified wild-type and two mutants representative of the blue shifted (Y95F) and red shifted (D212N/F234S) PR at acidic (A) and alkaline (B) pH. Microbial rhodopsins in general exhibit two spectral forms in a proton dependent equilibrium and absorption maximum of each pigment was measured in acidic (pH 4.0) and alkaline (pumping) state (pH 10.0). The absorption maxima in acidic state are 548 nm (wild type), 524 nm (Y95F), and 562 nm (D212N/F234S), and in the alkaline state they are 520 nm (wild-type), 513 nm (Y95F), and 537 nm (D212N/F234S).

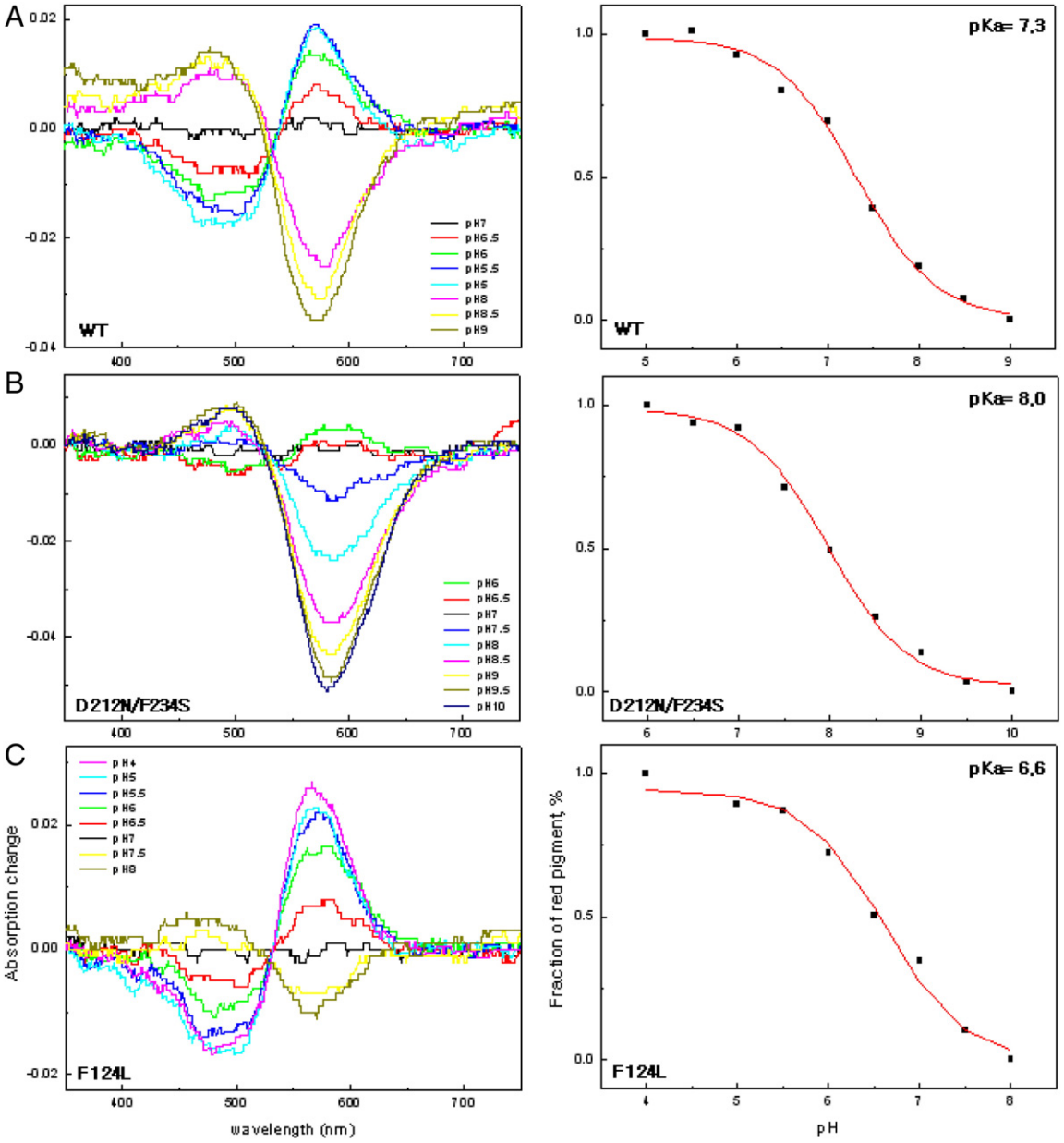

Fig. 5. pH dependencies of the relative concentration of acid versus alkaline forms of the wild-type (A), D212N/F234S (B), and F124L (C) pigments. Difference spectra were constructed using the spectrum at pH 7.0 as the reference. The pH of purified His-tagged PR in 50 mM Tris, 150 mM NaCl, 1% DDM was adjusted with dilute NaOH or HCl. pH titration curves indicate the relative concentration of acid (protonated) form of the pigments. This figure shows only three examples of typical pK_a values, one for the wild-type, one of the pigments with upshifted and one with downshifted counterion pK_a value (shown in the figure).

maximum of G70D was blue-shifted about 5 nm compared to that of the double mutant (Table 1). But there was just 2 nm difference in the absorption maximum position between the wild-type and G70D mutant at pH 10.0. The expression level of G70D was much lower than for the wild-type, and it suggests that the mutation at this position could cause the protein instability. According to the sequence alignment of PR and BR [1,2], the side chain of T44 in helix A forms a bridge that packs against the groove created by G66 and G70 in helix B. Mutation at the G70 position may disrupt this helix-helix interaction [29,30].

The apparent color of L67R (in helix B) pigment expressed in *E. coli* was yellow (see above for the possible reasons) but that of the purified pigment was purple (λ_{max} = 547 nm), red shifted about 30 nm from the wild-type. Expression level of this mutant was also very low, and the new positively charged residue seemed to influence the structural stability. But, the pK_a value of this mutant was just 0.3 pH units different from that of the wild-type.

3.2.2. Mutations in the helices C to F

Most of the color-changing mutations occurred in the helices C and D (12 out of 20 mutated residues), and four mutations were in the conserved retinal binding pocket (Fig. 3) [1,2]. The color of the purified T91I was red at pH 7.0 (Fig. 2B), but the absorption maximum was just 2 nm blue-shifted (518 nm) from that of the wild-type at high pH. This difference can be explained by the larger spectral shift in the acidic form (Table 1) affecting the color of the mixture of acidic and alkaline species at pH 7.

The expression level of Y95F/C156R double mutant was very similar to the wild-type, but this mutant was not able to produce a colored pigment. It seemed that the replacement of C156 with positively charged residue was responsible for this phenotype (it is known that all cysteines in PR can be replaced by neutral residues without major effects). The apparent color of the C156R mutant in the membrane was yellow and the amount of purified pigment was very low. We concentrated one liter culture to 1 mL in DM for measuring

the spectrum of C156R. Absorption maximum of the purified protein was the same as in the wild-type, but the pK_a value was a little bit lower (Table 1). The Y95 residue is conserved in the most of microbial rhodopsins [1–3]. The Y95F mutant (red colored pigment) has a blue shifted spectrum (λ_{max}=513 nm), similar to the Y83F mutant of bacteriorhodopsin [31]. Elimination of the hydroxyl group of Y95 may have influenced the ring of the retinal through the change in hydrophilicity of the environment.

W98 is located in the retinal binding pocket, and is conserved among microbial rhodopsins [1,2], being located next to the primary proton acceptor D97. W98G mutation was responsible for the phenotype of the double mutant W98G/V136M. W98G and the double mutant both showed blue shifted absorption spectra (λ_{max}=493 nm and 509 nm in the alkaline form, respectively). The position of W98 in PR is homologous to that of W86 in BR [32]. In the 3D structure model, W86 in BR is shown on the hydrophilic surface of helix C, facing the retinal chromophore inside the seven helical bundle. The decreased steric hindrance in the W98G mutant seemed to induce the blue shifted spectrum. In the case of W98G, absorption maximum of the pumping state was determined at pH 9.0 because it was photobleached at pH over 9.0. Interestingly, its color disappeared under the illumination in a few minutes and returned in the dark in a several minutes as well, probably due to the formation of long-living M-like products known for other retinal proteins. Thus, we had to measure the difference spectra at each pH with at least ten minute intervals.

Violet colored T101A/I194N pigment had about 20 nm red shifted λ_{max}, similar to T101A. T101 is one of the retinal binding pocket residues and is conserved in the most of microbial rhodopsins [1,2]. T101A/I194N protein precipitated in 0.02% DDM, and we had to use 0.1% DDM to solubilize this mutant. Absorption maximum of the double mutant was 5 nm more red shifted than in T101A, and the pK_a value was somewhat higher (Table 1). This showed that the effect on the spectrum comes mainly from the T101A mutation, but the effect on the pK_a may come from both T101A and I194N. Indeed, although the difference of absorption maxima between the wild-type and I194N was very small, the counterion pK_a of the mutant is upshifted. T101 in PR has the same position as T89 in BR. T89 of BR is close to the retinal and stabilizes the energetically unfavorable ionized state of the Schiff base-proton acceptor, D85 [33,34].

V102 residue is located in the retinal binding pocket as well, and BR has a threonine residue instead of valine at this position. We had two mutations of this residue, V102D and V102A. In the case of V102D, absorption maximum was similar to the wild-type but we confirmed that the color of the pigments in the membrane is slightly different (not shown). It seems to be because of the low expression level of the protein. Absorption maxima of these two V102 mutants were slightly blue-shifted and the pK_a value of V102D was downshifted (Table 1). According to previous research, T90 in BR plays a role in the protein structural stability through hydrogen bond to D115 and steric contact with the retinal [34,35]. In PR, it seems that the different absorption maximum was caused by change in a steric contact, because the larger blue shift of the absorption maximum resulted from the removal of bulky side chain in V102A, but not in V102D. In any case, the interaction similar to T90-D115 hydrogen bonding of BR cannot be important for PR, as this pair is represented by Val and Ser.

C107 residue is located next to the proton donor E108. C107R mutant protein precipitated in 0.02% DDM as well, and we had to use 0.05% DDM to solubilize it. This mutant showed red shifted absorption spectrum (540 nm) and the pK_a value was significantly higher than in the wild-type.

F124 residue is located at the end of the helix D, close to the cytoplasmic side, far from the retinal binding region. Surprisingly, a mutation at this position, F124L, induced the color change. Absorption maximum of F124L was 4 nm red shifted from that of the wild-type and the pK_a value was lower than that for the wild-type (Fig. 5C). Interestingly, this residue is represented by an aliphatic amino acid in BR, halorhodopsin, SR-I, and *Anabaena* sensory rhodopsin (ASR) [2], all of which are red-shifted compared to PR.

The K126R/Y200H double mutant had 18 nm blue shifted absorption spectra and the counterion pK_a value similar to WT. These spectral characteristics of the double mutant (K126R/Y200H) were close to those of Y200H but not of K126R, even though not exactly the same. It seems that the effects of each mutation are additive. Y200 is another retinal binding pocket residue. The counterion pK_a value of Y200H mutant was almost the same as in the wild-type, however, this mutant had a highly blue shifted absorption maximum (497 nm). Another Y200 mutant, Y200N, showed the spectral properties similar with those of Y200H, as its absorption maximum was also blue shifted. But the pK_a value determined in Y200N was higher than that

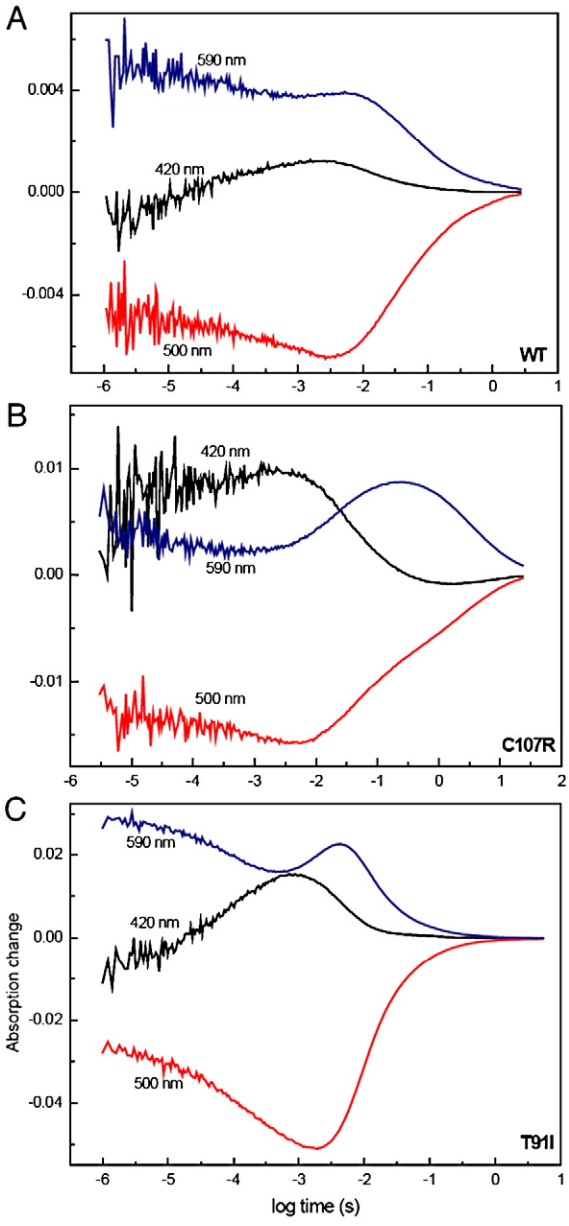

Fig. 6. Photocycle measurements of the wild type and two characteristic mutant PRs in DDM-treated membranes encased in polyacrylamide gel at 22 °C. Absorption changes after a laser pulse were followed at 420, 500, and 590 nm, and are shown on a logarithmic time-scale. The photocycle properties were different for each mutant, but most of the red shifted pigments had slow M (420 nm) and O (590 nm) decays, aswell as the K=M equilibrium shifted towards M. Lower proton pumping activity of those mutants can be correlated with slower decay rates of the late photointermediates. A. WT; B. Typical slow-cycling red-shifted mutant, C107R; C. Typical fast-cycling mutant, T91I.

of Y200H. Y200 is a homolog of Y185 in BR. The Y185F mutant in BR was shown to have red shifted absorption maximum when expressed in *E. coli* [36], and exists as a mixture of unshifted and strongly red-shifted acidic species when expressed in *H. halobium* [37]. On the contrary, in PR, the eliminated hydroxyl group caused blue shifted absorption maximum, pointing at a different hydrogen-bonding geometry of the active center, as also suggested from the FTIR studies [38,39].

The apparent color of G138D and M140K proteins was yellow in the membrane but purified proteins showed colored pigments in 0.02% DDM (Fig. 2B). When they were expressed in *E. coli* strain UT5600 with exogenous all-*trans* retinal, the color of proteins was like that of purified pigments (not shown). The pK_a values of the two mutants were slightly different from the wild-type, but the absorption maximum was changed substantially in one of them. While M140K spectrum was similar to the wild-type, the G138D mutant was blue shifted (Table 1). Although M140K was similar to the wild type, it probably showed a different apparent color because the expression level of the protein was low. Since the G138D mutant photobleached at pH over 9.0, the absorption maximum of the pumping state was determined at pH 9.0. At low pH, the short-wavelength species (possibly, with 9-*cis*-retinal) were formed for G138D, similar to what was described for the D227N mutant [40]. This residue (G138) is conserved in the most of microbial rhodopsins and may be important for the structural stability.

The absorption maximum of D212N/F234S was nearly 20 nm red shifted and the phenotype was the same as that of the F234S mutant. In addition, the counterion pK_a values of F234S and the double mutant were almost the same, higher than in the wild-type. It looks that the D212N replacement did not strongly contribute to the phenotype of the double mutant. In fact, the absorption maximum of D212N was similar to the wild-type, even though the counterion pK_a value was somewhat lower.

3.3. Photochemical characteristics of color-tuning mutants

Previous work has shown that PR functions as a light-driven proton pump [3,4,17,18,27]. For measuring proton transport activity, we made *E. coli* right-side-out vesicles [27] containing each mutant and the wild-type PR. Pumping activity of each mutant was evaluated by measuring pH difference in the presence and the absence of light passed through the short wavelength cutoff filter (>440 nm), and the difference of pH was converted into the number of transported protons using the subtraction of small gradual base-line shifts from *E. coli* membrane without rhodopsin. All the mutants and wild-type PR were capable of proton pumping upon the illumination, but the proton transport activity of almost all of the mutants was lower than

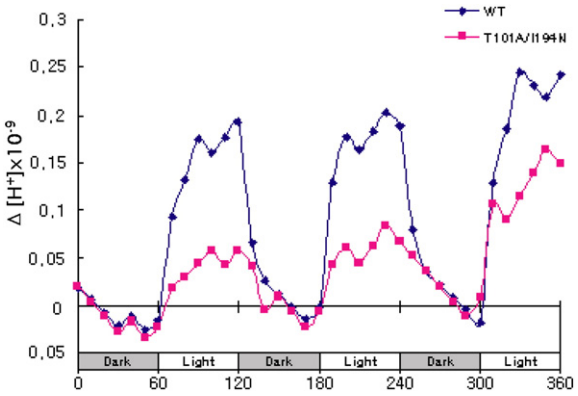

Fig. 7. Light induced proton fluxes in right-side-out vesicles containing the wild type (blue), and T101A/I194N (pink) PR. Initial pH values were adjusted to 9.0 and base line shifts were subtracted. Proton flux of T101A/I194N is about 30% of that of the wild type.

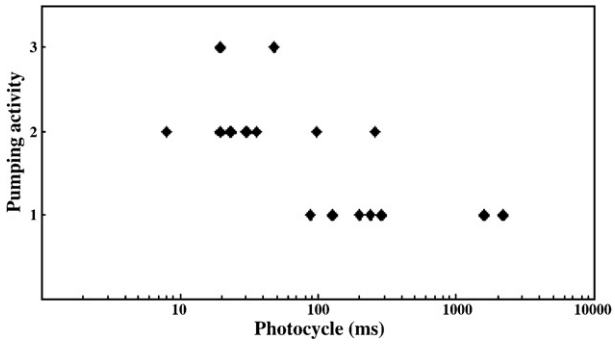

Fig. 8. A relationship between proton pumping activity and the photocycle turnover (given as a half-time). There is a positive correlation between pumping activity and the photocycle rate. Mutants with rapid photocycle turnover (the O decay) generally show good pumping activity. The scale 1, 2, 3 means (+), (++), and (+++) as described in Table 1.

for the wild-type (Table 1). Fig. 6 shows an example of measurement of the pumping activity of the wild-type and of a representative mutant.

Similar to other ion transporting rhodopsin, major BR-like photointermediates were identified in proteorhodopsin [17,19,20]. The M and O intermediates of each mutant were compared in this study. The photocycles could not be detected for several yellow pigments, as D24V/G70D, G70D, W98G/V136M, and W98G mutants were photobleached. Thus, the photocycles were measured just for 19 mutants (Table 1).

Like other transport rhodopsins, the wild-type MBP possesses a fast photocycle [1–3], but the photocycling rates of the mutants were very diverse. Fig. 7 shows the photocycle of the wild-type PR and characteristic mutants with faster and slower photocycling rates compared to that of the wild-type. The single mutants D24V, V136M, and I194N, which did not contribute appreciably to the spectrally changed phenotypes of the studied double mutants, demonstrated normal photocycles (Table 1).

Several red shifted mutants, T101A, C107R, Y200N, and F234S, showed the same photochemical properties, having higher M state accumulation due to the K=M equilibrium shift and slower M and O decays. On the contrary, blue-shifted Y95F had almost no M accumulation, even though the O intermediate and proton pumping were observed, similar to several cases in BR where M did not accumulate for kinetic reasons. T101A/I194N and D212N/F234S were similar to T101A and F234S in that respect. Although BR homologs of some of these mutated residues are not directly involved in the proton transport pathway, their effect on the retinal influenced the proton transfers as well. Among those, T101 and Y200, residues in the retinal binding pocket of PR, are homologs of T89 and Y185 in BR. The hydrogen bonds between T89 and D85, and Y185 and D212 in BR are important for the protein stability and optimal proton transport. T101 and Y200 in PR may have the same roles as their homologs in BR, even though it was shown that T101 has interactions somewhat different from those in BR [39].

The photocycle properties seemed to be correlated with the proton pumping activity. For example, most of the red shifted PR mutants had slow M and O decay and a poor pumping activity, mainly due to the slower photocycle turnover (Fig. 8).

4. Discussion

Spectral tuning is crucial for microbial rhodopsins due to the great variety in host habitats and protein functions [2]. In PR, it was found that L105 residue is the major determinant of the spectral tuning [8,27], but recent evolutionary analysis suggests that other residues may be involved as well [10]. To identify additional residues involved in color determination, we isolated several mutants with changed

color using the *E. coli* rhodopsin expression system with endogenous retinal synthesis. The residues related to color-tuning can be expected to reside in the retinal binding pocket, but we found that some residues located far from the chromophore were able to affect the color of the protein as well. Random mutagenesis screening was very useful to find mutants with color changes, and visual inspection of the colored colonies proved to be surprisingly efficient in detecting even minor spectral differences, later confirmed by absorption spectroscopy. A certain number of internal stop codons and wobble sequence changes were also identified because the PR gene was randomly mutagenized by PCR. We were able to obtain 6.8% (53/775) of colonies with changed color on the plate. After the screening, we found 16 isolates out of the 22 colonies, where 20 single residues were responsible for these color changes, out of which 14 residues did not belong to the retinal binding pocket and only 4 residues did. There were two cases where two mutations involved the same residues — V102 and Y200. Six isolates were nonsense mutations which have stop codon in the middle of the gene. Interestingly, mutations in the primary proton acceptor D97 were not detected, but we realize that our method may not produce the exhaustive set of the color-changing residues.

Colonies with changed colors could be divided into two large groups, with different shades of reddish/bluish color or yellow. There are several possible reasons for formation of yellow colored colonies. Protein synthesis could be terminated by internal stop codon produced by the PCR random mutagenesis, PR could have a large blue shift of absorption spectrum, or have very low expression level. Thus, we further investigated 22 yellow colored isolates and found that 4 of them can form a pigment in DDM. Because of the low expression level, their color on the plate was masked by β-carotene.

In general, spectral tuning can result from effects of amino acids that directly interact with the retinal, or indirectly influence the retinal binding pocket, or influence the protein stability [9,10], or interaction between the helices, which is also a factor of spectral tuning [41]. Our results indicate that the spectral characteristics could be influenced by all of those effects.

Mutation of a single residue can influence many aspects of its phenotype. Thus, we measured the absorption spectra, pH-dependent difference spectra, rates of the photocycle intermediates, and proton pumping activity as characteristic properties. PR has two distinct spectral states differing in the protonation of the carboxylic proton acceptor D97 [19], similar to BR [42,43]. We compared all the spectral properties of mutants in the pumping state of protein at basic pH, and only absorption spectra at acidic pH (Table 1). The pH of the *E. coli* colony on screening plate is approximately 8.3 after 48 h of growth of streaked colony and that pH was above the pK_a values of almost all mutant proteins, making favorable conditions for isolation of the color-tuning mutants. Actually, these mutants have a chance to exist in the pumping state in the marine environment, with pH near or above 8.0 [44].

Previous work studied spectral properties of 21 different proteorhodopsins obtained from natural marine environment from a variety of places and depths [45]. It is known that there are two clusters of proteorhodopsin, GPR and BPR, and their spectral properties depend on the genomic variance optimized to match the depth of marine environment [4,10,45]. The amino acid sequence of those proteorhodopsins had above 80% identity and there were several residues different between GPR and BPR. Most of our color-tuning mutations involved residues conserved in the amino acid sequences of proteorhodopsins and just 4 mutation sites were at unexpected locations. Probably, most of marine proteobacteria containing these mutant proteorhodopsins would not be able to survive in the natural environment because of decreased ability to absorb prevalent wavelength of light and pump protons. The ability to convert solar energy to proton motive force is critical for obtaining energy [3,4,8], so proton pumping activity must be important for the survival of γ-proteobacteria. The ability to absorb light which is prevalent at the depth of the habitat is also important for survival. In this context, some of our red shifted mutant PRs such as T101A, V102A, C107R, K126R/Y200H, Y200N, and F234S, were not only disadvantaged spectrally, but also had a very slow photocycle and poor proton transport activity. It means that they cannot produce chemical energy of proton gradients efficiently and have very low probability of being found in nature.

In this study, we found several amino acid residues related to color-tuning of PR, including those beyond the retinal binding pocket, which could influence the retinal binding pocket residues indirectly, or affect folding and structural stability of the protein. Taking BR as an example, the future structural studies will provide the accurate location and role of each of these residues.

Acknowledgments

We thank Professors von Lintig and Vogt for providing two plasmids which contain carotenoid biosynthesis genes and mouse dioxygenase gene, and Professors John Spudich and Vishwa Trivedi for supporting preliminary work on the construction of the retinal producing plasmid.

References

[1] J.L. Spudich, C.S. Yang, K.H. Jung, E.N. Spudich, Retinylidene proteins: structures and functions from archaea to humans, Annu. Rev. Cell Dev. Biol. 16 (2000) 365–392.
[2] J.L. Spudich, K.H. Jung, in: W.R. Briggs, J.L. Spudich (Eds.), Microbial rhodopsins: phylogenetic and functional diversity, In Handbook of photosensory receptors, WILEY-VCH Verlag GmbH & Co. KGaA, Weinheim, 2005, pp. 1–23.
[3] O. Béjà, L. Aravind, E.V. Koonin, M.T. Suzuki, A. Hadd, L.P. Nguyen, S.B. Jovanovich, C.M. Gates, R.A. Feldman, J.L. Spudich, E.N. Spudich, E.F. Delong, Bacterial rhodopsin: Evidence for a new type of phototrophy in the sea, Science 289 (2000) 1902–1906.
[4] O. Béjà, E.N. Spudich, J.L. Spudich, M. Leclerc, E.F. DeLong, Proteorhodopsin phototrophy in the ocean, Nature 411 (2001) 786–789.
[5] G. Sabehi, R. Massana, J.P. Bielawski, M. Rosenberg, E.F. Delong, O. Béjà, Novel proteorhodopsin variants from the Mediterranean and Red Seas, Environ. Microbiol. 5 (2003) 842–849.
[6] J.C. Venter, K. Remington, J.F. Heidelberg, A.L. Halpern, D. Rusch, J.A. Eisen, D. Wu, I. Paulsen, K.E. Nelson, W. Nelson, D.E. Fouts, S. Levy, A.H. Knap, M.W. Lomas, K. Nealson, O. White, J. Peterson, J. Hoffman, R. Parsons, H. Baden-Tillson, C. Pfannkoch, Environmental genome shotgun sequencing of the Sargasso Sea, Science 304 (2004) 66–74.
[7] D.B. Rusch, A.L. Halpern, G. Sutton, K.B. Heidelberg, S. Williamson, S. Yooseph, D. Wu, J.A. Eisen, J.M. Hoffman, K. Remington, K. Beeson, B. Tran, H. Smith, H.B. Tillson, C. Stewart, J. Thorpe, J. Freeman, C.A. Pfannkoch, J.E. Venter, K. Li, S. Kravits, J.F. Heidelberg, T. Utterback, Y.H. Rogers, L.I. Falcon, V. Souza, G.B. Rosso, L.E. Eguiarte, D.M. Karl, S. Sathyendranath, T. Platt, E. Bermingham, V. Gallardo, G.T. Castillo, M.R. Ferrari, R.L. Strausberg, K. Nealson, R. Friedman, M. Frazier, J.C. Venter, The sorcerer II global ocean sampling expedition: northwest Atlantic through eastern tropical Pacific, PLoS Biol. 5 (3) (2007) e77.
[8] D. Man, W. Wang, G. Sabehi, L. Aravind, A.F. Post, R. Massana, E.N. Spudich, J.L. Spudich, O. Béjà, Diversification and spectral tuning in marine proteorhodopsins, EMBO J. 22 (2003) 1725–1731.
[9] K. Shimono, Y. Furutani, H. Kandori, N. Kamo, A pharaonis phoborhodopsin mutant with the same retinal binding site residues as in bacteriorhodopsin, Biochemistry 41 (2002) 6504–6509.
[10] J.P. Bielawski, K.A. Dunn, G. Sabehi, O. Béjà, Darwinian adaptation of proteorhodopsin to different light intensities in the marine environment, Proc. Natl. Acad. Sci. U. S. A. 101 (2004) 14824–14829.
[11] R.R. Birge, Nature of the primary photochemical events in rhodopsin and bacteriorhodopsin, Biochim. Biophys. Acta 1016 (1990) 293–327.
[12] M. Ottolenghi, M. Sheves, Synthetic retinals as probes for the binding site and photoreactions in rhodopsins, J. Membr. Biol. 112 (1989) 193–212.
[13] B. Yan, J.L. Spudich, P. Mazur, S. Vunnam, F. Derguini, K. Nakanishi, Spectral tuning in bacteriorhodopsin in the absence of counterion and coplanarization effects, J. Biol. Chem. 270 (1995) 29668–29670.
[14] J. von Lintig, K. Vogt, Vitamin A formation in animals: molecular identification and functional characterization of carotene enzymes, J. Nutr. 134 (2004) 251S–256S.
[15] G. Sabehi, A. Loy, K.H. Jung, R. Partha, J.L. Spudich, T. Isaacson, J. Hirschberg, M. Wagner, O. Beja, New insights into metabolic properties of marine bacteria encoding proteorhodopsins, PLoS Biol. 3 (8) (2005) e273.
[16] A. Martinez, A.S. Bradly, J.R. Waldbauer, R.E. Summons, E.F. Delong, Proteorhodopsin photosystem gene expression enable photophoshorylation in a heterologous host, Proc. Natl. Acad. Sci. U. S. A. 104 (2007) 5590–5595.
[17] T. Friedrich, S. Geibel, R. Kalmbach, I. Chizhov, K. Ataka, J. Heberle, M. Engelhard, E. Bamberg, Proteorhodopsin is a light-driven proton pump with variable vectoriality, J. Mol. Biol. 321 (2002) 821–838.

[18] A.K. Dioumaev, J.M. Wang, Z. Bálint, G. Váró, J.K. Lanyi, Proton transport by proteorhodopsin requires that the retinal Schiff base counterion Asp-97 be anionic, Biochemistry 42 (2003) 6582–6587.
[19] A.K. Dioumaev, L.S. Brown, J. Shih, E.N. Spudich, J.L. Spudich, J.K. Lanyi, Proton transfers in the photochemical reaction cycle of proteorhodopsin, Biochemistry 41 (2002) 5348–5358.
[20] G. Varo, L.S. Brown, M. Lakatos, J.K. Lanyi, Characterization of the photochemical reaction cycle of proteorhodopsin, Biophys. J. 84 (2003) 1202–1207.
[21] S.J. Giovannoni, L. Bibbs, J.C. Cho, M.D. Stapels, R. Desiderio, K.L. Vergin, M.S. Rappé, S. Laney, L.J. Wilhelm, H.J. Tripp, E.J. Mathur, D.F. Barofsky, Proteorhodopsin in the ubiquitous marine bacterium SAR11, Nature 438 (2005) 82–85.
[22] L. Gomez-Consarnau, J.M. González, M.C. Lladó, P. Gourdon, T. Pascher, R. Neutze, C.P. Alió, J. Pinhassi, Light stimulates growth of proteorhodopsin-containing marine flavobacteria, Nature 445 (2007) 210–213.
[23] J. von Lintig, K. Vogt, Filling the gap in vitamin A research, J. Biol. Chem. 275 (2000) 11915–11920.
[24] R.C. Cadwell, G.F. Joyce, Randomization of genes by PCR mutagenesis, PCR Methods Appl. 2 (1992) 28–33.
[25] K.H. Jung, J.L. Spudich, Suppressor mutation analysis of the sensory rhodopsin I-transducer complex: insights into the color-sensing mechanism, J. Bacteriol. 180 (1998) 2033–2042.
[26] S.N. Ho, H.D. Hunt, R.M. Horton, J.K. Pullen, L.R. Pease, Site-directed mutagenesis by overlap extension using the polymerase chain reaction, Gene (Amst) 77 (1989) 51–59.
[27] W.W. Wang, O.A. Sineshchekov, E.N. Spudich, J.L. Spudich, Spectroscopic and photochemical characterization of a deep ocean proteorhodopsin, J. Biol. Chem. 278 (2003) 33985–33991.
[28] S.A. Waschuk, A.G. Bezerra Jr., L. Shi, L.S. Brown, *Leptosphaeria* rhodopsin: bacteriorhodopsin-like proton pump from a eukaryote, Proc. Natl. Acad. Sci. U. S. A. 102 (2005) 6879–6883.
[29] M. Mottamal, T. Lazaridis, The contribution of Ca–H–O hydrogen bonds to membrane protein stability depends on the position of the amide, Biochemistry 44 (2005) 1607–1613.
[30] K.R. Mackenzie, J.H. Prestegard, D.M. Engelman, A transmembrane helix dimer: structure and implications, Science 276 (1997) 131–133.
[31] E.S. Imasheva, M. Lu, S.P. Balashov, T.G. Ebrey, Y. Chen, Z. Ablonczy, D.R. Menick, R.K. Crouch, Exploring the function of Tyr83 in bacteriorhodopsin: Features of the Y83F and Y83N mutants, Biochemistry 40 (2001) 13320–13330.
[32] T. Mogi, T. Marti, H.G. Khorana, Structure–function studies on bacteriorhodopsin: IX. Substitutions of tryptophan residues affect protein–retinal interactions in bacteriorhodopsin, J. Biol. Chem. 264 (1989) 14197–14201.
[33] H. Luecke, H.T. Richter, J.K. Lanyi, Proton transfer pathways in bacteriorhodopsin at 2.3 angstrom resolution, Science 280 (1998) 1934–1937.
[34] H. Kandori, N. Kinoshita, Y. Yamazaki, A. Maeda, Y. Shichida, R. Needleman, J.K. Lanyi, M. Bizounok, J. Herzfeld, J. Raap, J. Lugtenburg, Local and distant protein structural changes on photoisomerization of the retinal in bacteriorhodopsin, Proc. Natl. Acad. Sci. U. S. A. 97 (2000) 4643–4648.
[35] A. Peralvarez-Marin, M. Marquez, J.L. Bourdelande, E. Querol, E. Padros, Thr-90 plays a vital role in the structure and function of bacteriorhodopsin, J. Biol. Chem. 279 (2004) 16403–16409.
[36] N.R. Hackett, L.J. Stern, B.H. Chao, K.A. Kronis, H.G. Khorana, Structure–function studies on bacteriorhodopsin. V. Effects of amino acid substitutions in the putative helix F, J. Biol. Chem. 262 (1987) 9277–9284.
[37] S. Sonar, M.P. Kreb, H.G. Khorana, K.J. Rothschild, Static and time-resolved absorption spectroscopy of the bacteriorhodopsin mutant Tyr-185–>Phe: evidence for an equilibrium between bR570 and an O-like species, Biochemistry 32 (1993) 2263–2271.
[38] V. Bergo, J.J. Amsden, E.N. Spudich, J.L. Spudich, K.J. Rothschild, Structural changes in the photoactive site of proteorhodopsin during the primary photoreaction, Biochemistry 43 (2004) 9075–9083.
[39] D. Ikeda, Y. Furutani, H. Kandori, FTIR study of the retinal Schiff base and internal water molecules of proteorhodopsin, Biochemistry 46 (2007) 5365–5373.
[40] E.S. Imasheva, S.P. Balashov, J.M. Wang, A.K. Dioumaev, J.K. Lanyi, Selectivity of retinal photoisomerization in proteorhodopsin is controlled by aspartic acid 227, Biochemistry 43 (2004) 1648–1655.
[41] K. Shimono, T. Hayashi, Y. Ikeura, Y. Sudo, M. Iwamoto, N. Kamo, Importance of the broad regional interaction for spectral tuning in *Natronobacterium pharaonis* phoborhodopsin (sensory rhodopsin II), J. Biol. Chem. 278 (2003) 23882–23889.
[42] J.K. Lanyi, Proton translocation mechanism and energetics in the light-driven pump bacteriorhodopsin, Biochim. Biophys. Acta 1183 (1993) 241–261.
[43] G. Varo, J.K. Lanyi, Photoreactions of bacteriorhodopsin at acid pH, Biophys. J. 56 (1989) 1143–1151.
[44] T. Clayton, R.H. Byrne, Spectrophotometric seawater pH measurements: total hydrogen ion concentration scale calibration of m-cresol purple and at-sea results, Deep-Sea Res. 40 (1993) 2115–2129.
[45] B.R. Kelemen, M. Du, R.B. Jensen, Proteorhodopsin in living color: diversity of spectral properties within living bacterial cells, Biochem. Biophys. Acta 1618 (2003) 25–32.